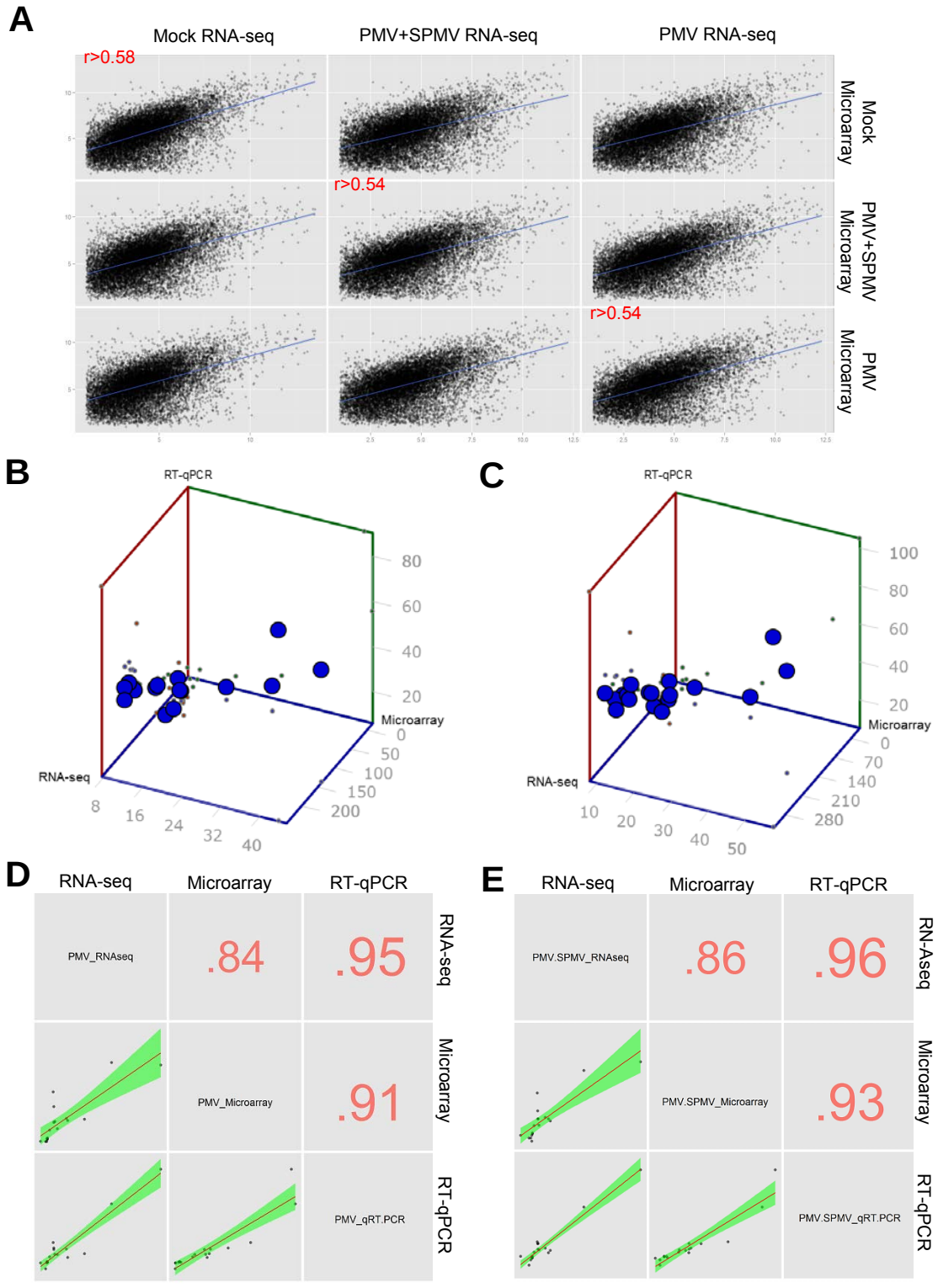

Supplemental Figure 1. Validation of RNA-seq expression data. (A) Expression of ~11,500 gene models as determined by RNA-seq (FPKM ≥2) was compared to their corresponding expression in microarrays (Mandadi and Scholthof, 2012). Pearson product-moment correlation coefficient (r) values of RNA-seq and micorarray data was >0.54, indicating a high degree of correlation. Fold-change expression of 18 genes mis-expressed in (B) PMV-, and (C) PMV+SPMV-infection relative to mock, determined using RNA-seq, microarray and RT-qPCR analysis, were clustered in a multivariate three-dimensional scatter plot. (D, E) The "r" coefficient values for bivariate comparisons between the three datasets show strong correlation between RNA-seq, microarray and RT-qPCR results. Together, these analyses support the use of RNA-seq methodology for transcriptome analysis, and revealed strong correlation with RT-qPCR and the microarray-based analysis.

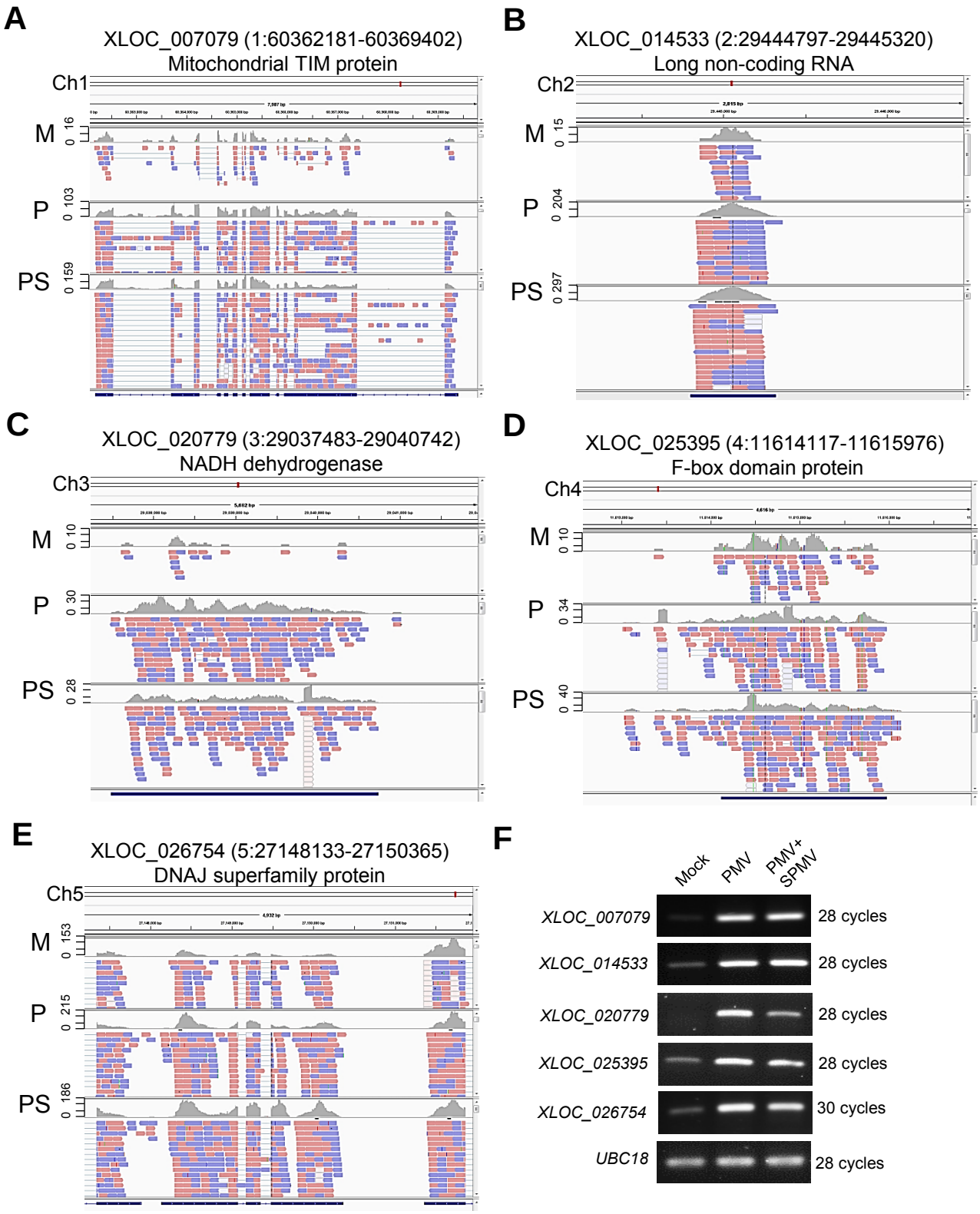

Supplemental Figure 2. Select examples of novel gene loci activated in virus-infected Brachypodium. Read densities (y-axis) of (A) XLOC_007079, (B) XLOC_014533, (C) XLOC_020779, (D) XLOC_025395 and (E) XLOC_026754 in mock (M), PMV (P) and PMV+SPMV (PS) are plotted against predicted gene models (x-axis) using the Integrative Genomics Viewer (IGV) visualization tool. Chromosomal loci and predicted BLASTX match (E-value cutoff: 1e-10) of the novel genes are indicated on top of each IGV panel. (F) RT-PCR analysis was performed to validate the expression of the selected novel genes induced in PMV- and PMV+SPMV-infected plants. *UBC18* was used as control for approximately equal cDNA amounts among the samples.

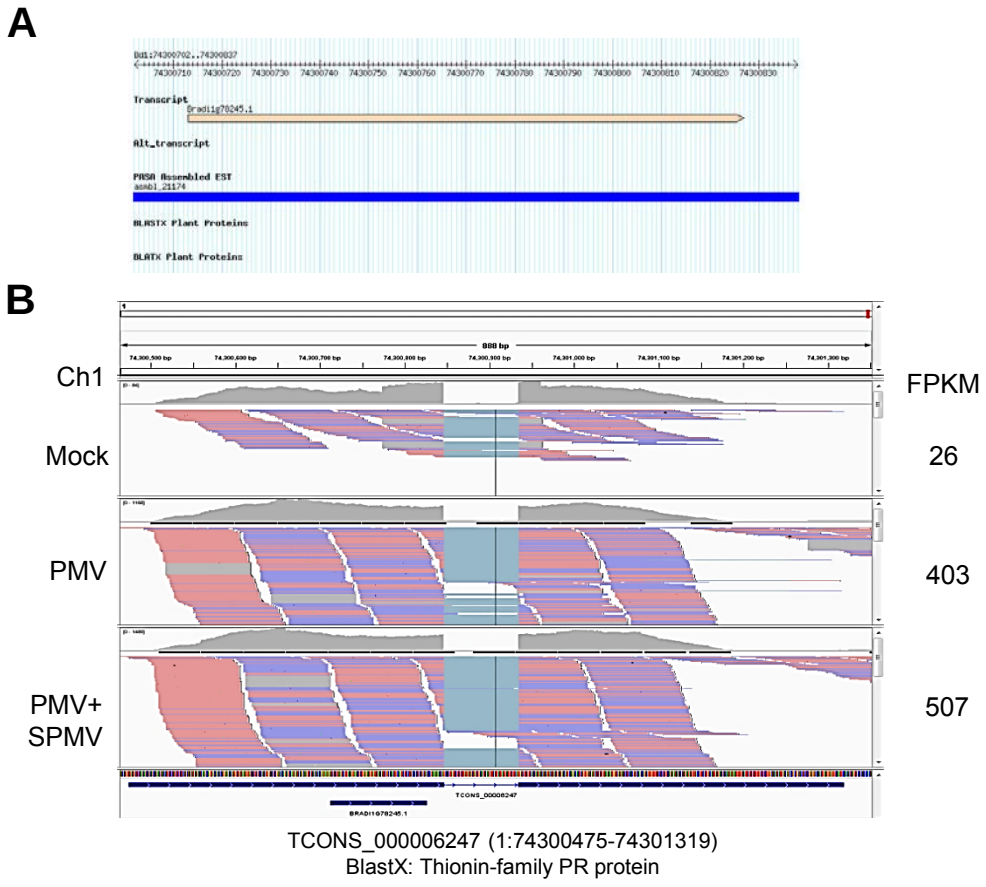

Supplemental Figure 3. Select example of a novel splice junctions identified in the RNA-seq analysis. (A) Brachypodium reference gene model for Bradi1g78245.1 showing a single exon encoding a protein with no predicted functions. (B) Cufflinks-assembled transcript model for Bradi1g78245. Read coverage (y-axis) of Bradi1g78245 in mock, PMV- and PMV+SPMV-infected samples was plotted against predicted Cufflinks transcript model and splice junctions (x-axis) using Integrative Genomics Viewer. The chromosomal locus of the novel transcript model is indicated at the bottom. BLASTX analysis (E-value: 1e-10) revealed this gene to encode a thionin-family Pathogenesis Related (PR) protein.

Mandadi and Scholthof (2015) Plant Cell 10.1105/tpc.114.133991

Supplemental Table 1. Cloning and sequencing of Bd-*SCL33* splice-variants.

Splice variant ID	Transcript length (nt)	Splicing pattern	Predicted protein (aa)
7	3048	Full-length pre-mRNA	9
6	2417	Intron3 retention (nt 1-496) + Intron1 retention (nt 1-872)	9
5	1545	Intron3 retention (nt 1-496)	75
4	1315	Intron3 retention (nt 231-496)	78
3	1157	Intron3 retention (nt 231-338)	78
Bradi1g61330.2	1049	Bradi1g61330.2	219
Bradi1g61330.1	1135	Primary transcript	246

Mandadi and Scholthof (2015) Plant Cell 10.1105/tpc.114.133991

Supplemental Table 2. Cuffcompare summary of locus-level sensitivity and specificity match scores of the Cufflinks transcript assemblies to reference Brachypodium (Bd21 v1.2) assembly.

	Sn	Sp	fSn	fSp
Mock				
Base level	100	91.6	-	-
Exon level	100.5	88.9	100	90
Intron level	100	92.3	100	93.6
Intron chain level	96.5	74.6	100	88
Transcript level	96.9	74.1	93.5	71.5
Locus level	97.3	90.5	100	92.9
PMV				
Base level	100	91.1	-	-
Exon level	100.5	88.3	100	89.4
Intron level	100	92	100	93.2
Intron chain level	96.3	74.1	100	87.5
Transcript level	96.8	73.3	93.3	70.7
Locus level	97.1	90	100	92.4
PMV+SPMV				
Base level	100	90	-	-
Exon level	100.7	87.3	100	88.4
Intron level	100	91.6	100	92.9
Intron chain level	96.4	72.2	100	85.3
Transcript level	96.9	71.2	93.5	68.7
Locus level	97.3	89.2	100	91.5

Sn-Sensitivity, Sp-Specificity, fSn-fuzzy sensitivity, fSp-fuzzy specificity

Mandadi and Scholthof (2015) Plant Cell 10.1105/tpc.114.133991

Supplemental Table 3. Primers used in this study.

Primer	Sequence (5' to 3')
XLOC_007079 Forward	TGCGACAGAAGGATGCTGAA
XLOC_007079 Reverse	GTCAGGATGGCTCACCCAAA
XLOC_014533 Forward	TATTTCTTCCCCTGCCCCCT
XLOC_014533 Reverse	GGCTTGTAGGCGCACAAAAT
XLOC_020779 Forward	TGAAGTAATGCGAGCGTGGT
XLOC_020779 Reverse	ACGGCTGAGTCGATTCTTGG
XLOC_025395 Forward	TAGCAACCCACGTTCCAACC
XLOC_025395 Reverse	ACTTTGGCAAGTCCGTCGAT
XLOC_026754 Forward	AAGCTTCCCACCATTCGGG
XLOC_026754 Reverse	TACAGGTCGTACTCCGTCGT
Bradi1g61330 Forward	CCTGTCCAAGCAGTACGCAG
Bradi1g61330 Reverse	GGAATAGAGCGCAGCACAG
Bradi4g00660 Forward	ACAGCAATGGCCACATCTGTTTAG
Bradi4g00660 Reverse	TTGTCTTGCGGACGTTGCTTTG